Homo- and Hetero-Stereocomplexes of Substituted Poly(lactide)s as Promising Biodegradable Crystallization-Accelerating Agents of Poly(L-lactide)

Hideto Tsuji, Satomi Yamamoto, Ayaka Okumura

Department of Environmental and Life Sciences, Graduate School of Engineering, Toyohashi University of Technology, Tempaku-cho, Toyohashi, Aichi 441-8580, Japan

Received 2 December 2010; accepted 14 January 2011
DOI 10.1002/app.34163
Published online 21 April 2011 in Wiley Online Library (wileyonlinelibrary.com).

ABSTRACT: Accelerated crystallization of poly(L-lactide) (PLLA) homo-crystallites occurred in the presence of poly(L-2-hydroxybutyrate) [P(L-2HB)], poly(D-2-hydroxybutyrate) [P(D-2HB)], and the mixture of P(L-2HB) and P(D-2HB) [P(L-2HB)/P(D-2HB)]. The accelerating effect of incorporated polymers decreased in the following order: P(L-2HB)/P(D-2HB) > P(D-2HB) > P(L-2HB) > none, for heating and isothermal crystallization for T_c of 130 and 135°C and P(D-2HB) > P(L-2HB)/P(D-2HB) > none > P(L-2HB), for cooling. The P(L-2HB)/P(D-2HB) homo-stereocomplex (HMSC) crystallites, P(D-2HB)/PLLA hetero-stereocomplex (HTSC) crystallites, and P(L-2HB) or P(D-2HB) homo-crystallites are found to be promising biodegradable nucleating agents for PLLA homo-crystallization. The P(L-2HB)/P(D-2HB) HMSC crystallites are most effective during isothermal crystallization and nonisothermal crystallization with heating, whereas the P(D-2HB)/PLLA HTSC crystallites are most effective during nonisothermal crystallization with cooling from the melt. In addition to the nucleating effect, the plasticizing effect of free P(2HB) chains increases both G and the PLLA spherulite number per unit mass. These effects result in accelerated crystallization of PLLA homo-crystallites. © 2011 Wiley Periodicals, Inc. J Appl Polym Sci 122: 321–333, 2011

Key words: biodegradable polyesters; poly(L-lactic acid); stereocomplex; nucleating agents

INTRODUCTION

Poly(L-lactide), that is, poly(L-lactic acid) (PLLA) is a plant-derived biodegradable polymer that is widely used as an alternative to petroleum-derived polymers.[1] The heat resistance of polymeric materials can be improved by increasing their crystallinity. It is important to achieve the acceleration of PLLA crystallization in the presence of nucleating agents or crystallization-accelerating agents, because, by using these agents, PLLA materials with high heat resistance can be produced in a short period of time, that is, at a reduced cost. Although numerous inorganic substances such as talc, montmorillonite, and nanostructured carbon[2–22] and low-molecular-weight organic compounds such as amide and hydrazide[23–26] are reported to act as nucleating agents of PLLA, only a few biodegradable nucleating agents have been reported so far.[4,13,27–31] The reported examples are homo-stereocomplex (HMSC) crystallites of PLLA/poly(D-lactide) (PDLA), which are formed upon addition of PDLA to PLLA[4,13,27–31] and polyglycolide,[31,32] which have a melting temperature (T_m) in the range of 220–230°C; these temperatures are much higher than that of PLLA (170–180°C). By using these biodegradable nucleating agents, completely biodegradable PLLA-based materials for biomedical, pharmaceutical, and environmental applications can be prepared. In addition, poly(D-3-hydroxybutyrate) and poly(ε-caprolactone) can accelerate the crystallization of PLLA by increasing the radial growth rate of spherulites (G) and the spherulite number per unit mass, respectively.[32]

PLLA/PDLA HMSC has been intensively studied for improving the mechanical and thermal properties and hydrolytic degradation resistance of PLLA-based materials.[33–38] On the other hand, poly(L-2-hydroxybutyrate) [P(L-2HB)], that is, poly(L-2-hydroxybutanoic acid) and poly(D-2-hydroxybutyrate) [P(D-2HB)], that is, poly(D-2-hydroxybutanoic acid) are biodegradable polymers and have the structure of PLLA and PDLA, which methyl groups are substituted by ethyl groups. Recently, HMSC formation between P(L-2HB) and P(D-2HB)[39] and hetero-stereocomplex (HTSC) formation between D-configured PDLA and L-configured P(L-2HB) and between L-configured PLLA and D-configured P(D-2HB)[40] were reported. Because of the

Correspondence to: H. Tsuji (tsuji@ens.tut.ac.jp).
Contract grant sponsor: Japan Society for the Promotion of Science; contract grant number: Grant-in-Aid for Scientific Research, Category "C", No. 16500291.

high-T_m values of these stereocomplexes at 198–212 and 170–184°C,[39,40] they can act as biodegradable nucleating agents for PLLA. Based on these facts, we investigated the effectiveness of the P(L-2HB)/P(D-2HB) HMSC and P(D-2HB)/PLLA HTSC as nucleating agents or crystallization-accelerating agents for PLLA homo-crystallites by the use of differential scanning calorimetry (DSC) and polarized optical microscopy. It was first found that these two stereocomplexes of substituted poly(lactide)s can act as promising biodegradable nucleating agents or crystallization-accelerating agents for PLLA homo-crystallites to prepare all biodegradable PLLA-based materials.

EXPERIMENTAL

Materials

PLLA was kindly supplied by Unitika Co. (Kyoto, Japan) and was purified by previously reported methods.[13,14,18] The purified PLLA [number–average molecular weight (M_n) = 9.5×10^4 g mol^{-1}, weight–average molecular weight (M_w)/M_n = 1.8, specific optical rotation in chloroform ($[\alpha]^{25}_{589}$) = −141 deg dm^{-1} g^{-1} cm^3] was dried *in vacuo* for at least 7 days. P(L-2HB) ($M_n = 3.3 \times 10^3$ g mol^{-1}, M_w/M_n = 3.9) and P(D-2HB) ($M_n = 3.6 \times 10^3$ g mol^{-1}, M_w/M_n = 3.7) were synthesized by polycondensation of L-[or (S)-] and D-[or (R)-]2-hydroxybutanoic acids (hydroxybutyric acids) (≥97.0%, enantiomeric ratio ≥99 : 1, Sigma-Aldrich Co.), respectively,[41] and purified[42] according to the method described in the previous literature.

In the present study, PLLA films with no incorporated polymer, with 10 wt % P(L-2HB), with 10 wt % P(D-2HB), and with 5 wt % P(L-2HB) and 5 wt % P(D-2HB) [abbreviated as P(L-2HB)/P(D-2HB)] were prepared. For the preparation of these specimens, each polymer solution (prepared separately) was mixed and cast onto Petri dishes, and the solvent (dichloromethane) was allowed to evaporate at 25°C for ~ 2 days. The specimens thus obtained were further dried *in vacuo* for at least 7 days. For the preparation of melt-quenched specimens, each of the as-cast films was packed in a DSC aluminum cell, sealed in a test-tube under reduced pressure, melted at 200°C for 3 min, and quenched at 0°C for 5 min.

Measurements and observations

The nonisothermal crystallization of the specimens (sample weight: ~ 3 mg) was monitored during heating and cooling using a Shimadzu (Kyoto, Japan) DSC-50 differential scanning calorimeter with a cooling cover (LTC-50) under nitrogen gas flow. To monitor the crystallization during heating, the melt-quenched specimens were heated at a rate of 10°C min^{-1} from 0 to 200°C. To trace the crystallization during cooling from the melt, the as-cast films were heated at a rate of 10°C min^{-1} from room temperature to 200°C, held at this temperature for 3 min, and then cooled at a rate of −1°C min^{-1} (crystallization was observed during cooling).

Spherulite growth in the specimens during isothermal crystallization was observed using an Olympus (Tokyo, Japan) polarization optical microscope (BX-50) equipped with a heating-cooling stage and a temperature controller (LK-600 PM, Linkam Scientific Instruments, Surrey, UK) under constant nitrogen gas flow. The as-cast specimens were first heated at a rate of 100°C min^{-1} from room temperature to 200°C, held at this temperature for 3 min, then cooled at a rate of −100°C min^{-1} to a crystallization temperature (T_c) in the range of 90–135°C, and held at the same T_c (spherulite growth was observed). The overall crystallization behavior of specimens during isothermal crystallization was monitored by measuring the light intensity transmitted through the specimens using the polarization optical microscope (BX-50) equipped with an As One (Osaka, Japan) LM-332 photometer. The WAXS measurements of melt-quenched and slowly cooled specimens were carried out at 25°C with a Rigaku (Tokyo, Japan) RINT-2500 equipped with a Cu-Kα source (λ = 0.1542 nm), which was operated at 40 kV and 200 mA (Rigaku Co., Tokyo, Japan).

RESULTS

Nonisothermal crystallization

First, we investigated nonisothermal crystallization during heating from 0°C and cooling from the melt. The results, especially for the latter method, will give crucial information for the processing of PLLA materials. Figure 1 shows the DSC thermograms of the melt-quenched and as-cast PLLA films with no incorporated polymer, P(L-2HB), P(D-2HB), and P(L-2HB)/P(D-2HB) during heating and cooling. During heating, the glass transition peak, cold crystallization peak, and melting peak of PLLA homo-crystallites were observed at around 60, 100, and 160°C, respectively, for all melt-quenched specimens. However, the PLLA film with P(L-2HB)/P(D-2HB) had an additional melting peak of P(L-2HB)/P(D-2HB) HMSC crystallites at around 210°C,[39] reflecting the presence of the HMSC crystallites. During cooling, the crystallization peak of PLLA homo-crystallites was observed in the temperature range of 90–130°C for all as-cast specimens, whereas the PLLA film with P(D-2HB) had an additional, broad exothermic peak at around 140°C. This broad exothermic peak is attributable to the crystallization of PLLA/P(D-2HB) HTSC crystallites. This is explained by the fact that the T_m of PLLA/P(D-2HB) HTSC (170–184°C)[40]

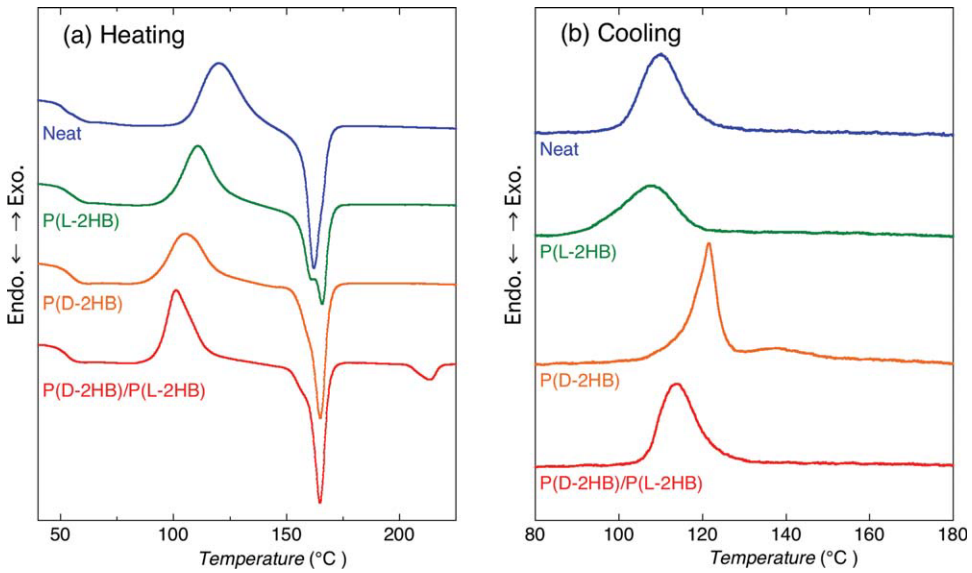

Figure 1 DSC thermograms of melt-quenched (a) and as-cast (b) PLLA films with no incorporated polymer, P(L-2HB), P(D-2HB), and P(L-2HB)/P(D-2HB) during heating from 0°C (a) and cooling from the melt (b), respectively. [Color figure can be viewed in the online issue, which is available at wileyonlinelibrary.com.]

is higher than that of PLLA homo-crystallites (~ 160°C, see Table I), which results in a larger supercooling effect ($\Delta T = T_m - T_c$, where T_c is the crystallization temperature) or crystallization driving force for the HTSC crystallites than the PLLA homo-crystallites at the same T_c values.

The onset, peak, and endset temperatures of (cold) crystallization [T_{cc}(O), T_{cc}(P), and T_{cc}(E), respectively] were estimated from the DSC thermograms (Fig. 1). Although the terms for cold crystallization temperature (T_{cc}) and enthalpy (ΔH_{cc}) are not suitable for describing cooling from the melt, we use these terms and abbreviations to discriminate them from crystallization temperature (T_c) for isothermal crystallization. T_{cc}(P) is the peak temperature for cold crystallization. T_{cc}(O) and T_{cc}(E) are the intersection temperatures of the base line and the tangent lines of the cold crystallization curves. In the case of heating, T_{cc}(O) and T_{cc}(E) are lower and higher than T_{cc}(P), respectively, whereas in the case of cooling, they are higher and lower than T_{cc}(P), respectively, as schematically shown in reported literature.[13,14,18]

TABLE I
Thermal Properties of Melt-Quenched and As-Cast PLLA Films with Different Incorporated Polymers during Heating from 0°C and Cooling from the Melt, Respectively

Incorporated polyester										
Type	Content (wt %)	Scanning direction	T_g[a] (°C)	T_{cc}(O)[b] (°C)	T_{cc}(P)[b] (°C)	T_{cc}(E)[b] (°C)	T_m[c] (°C)	Non-normalized ΔH_{cc}[d] (J g^{-1})	Normalized ΔH_{cc}[d] (J g^{-1})	ΔH_m[d] (J g^{-1})
Not added	0	Heating	47.9	105.8	120.0	138.5	162.1	32.5	32.5	31.4
P(L-2HB)	10		49.5	97.5	110.7	124.7	161.1, 165.7	27.2	30.2	27.2
P(D-2HB)			50.3	90.6	105.3	121.0	164.9	27.4	33.6	28.3
P(L-2HB)/ P(D-2HB)	5/5		48.8	92.9	101.0	116.4	164.9 (213.3)[e]	28.4	31.6	28.1 (3.5)[f]
Not added	0	Cooling	–	119.6	110.1	100.9	–	36.6	36.6	–
P(L-2HB)	10		–	118.8	107.6	92.4	–	31.1	34.6	–
P(D-2HB)			–	125.8	121.5	114.6	–	30.1	36.9	–
P(L-2HB)/ P(D-2HB)	5/5		–	123.3	113.5	106.4	–	35.8	39.8	–

[a] Glass transition temperature.
[b] T_{cc}(O), T_{cc}(P), and T_{cc}(E) are onset, peak, and endset temperatures of cold crystallization, respectively.
[c] Melting temperature of PLLA homo-crystallites.
[d] ΔH_{cc} and ΔH_m are the enthalpies of cold crystallization and melting of PLLA homo-crystallites, respectively.
[e] The value in parentheses is T_m of P(L-2HB)/P(D-2HB) HMSC crystallites.
[f] The value in parentheses is ΔH_m of P(L-2HB)/P(D-2HB) HMSC crystallites.

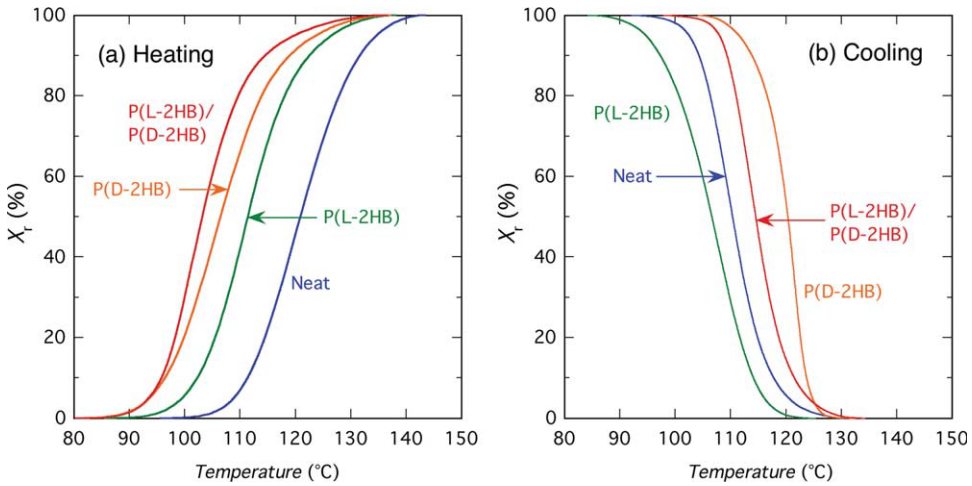

Figure 2 Relative crystallinity (X_r) of PLLA of melt-quenched (a) and as-cast (b) PLLA films with no incorporated polymer, P(L-2HB), P(D-2HB), and P(L-2HB)/P(D-2HB) during heating from 0°C (a) and cooling from the melt (b), respectively. [Color figure can be viewed in the online issue, which is available at wileyonlinelibrary.com.]

The ΔH_{cc} values were normalized by the weight fraction of crystallizable PLLA based on non-normalized ΔH_{cc} according to the following assumptions. In the case of the PLLA film with P(D-2HB), all the added P(D-2HB) chains are assumed to form HTSC with PLLA chains to the theoretically maximum extent (these PLLA chains are no longer crystallizable as PLLA homo-crystallites). In the PLLA film with P(L-2HB)/P(D-2HB), all the added P(2HB) chains are assumed to form P(L-2HB)/P(D-2HB) HMSC. However, in the PLLA film with P(L-2HB), PLLA and P(L-2HB) are thought to form their respective homo-crystallites. In the cases of PLLA films with P(L-2HB)/P(D-2HB) and P(L-2HB), PLLA chains with a weight fraction of 90 wt % are crystallizable as PLLA homo-crystallites. Based on these assumptions, normalized ΔH_{cc} values were calculated using the following equations:

$$\text{Normalized } \Delta H_{cc}\ (\text{J g}^{-1}) = \text{non-normalized } \Delta H_{cc}\ (\text{J g}^{-1}))/[1 - W_{P(2HB)}(\text{wt}\,\%)/100], \quad [\text{for PLLAfilms with P(L} - \text{2HB) and P(L} - \text{2HB)/P(D} - \text{2HB)}] \quad (1)$$

$$\text{Normalized } \Delta H_{cc}\ (\text{J g}^{-1}) = \text{non-normalized } \Delta H_{cc}\ (\text{Jg}^{-1})/[1 - (1 + 72.1/86.1) \times W_{P(2HB)}(\text{wt}\,\%)/100], \quad [\text{for PLLA film with P(D} - \text{2HB)}] \quad (2)$$

where $W_{P(2HB)}$ is the weight fraction of P(2HB), and the values 72.1 and 86.1 are the molecular weights of monomer units of PLLA and P(2HB), respectively. The recorded thermal properties of the PLLA films with no incorporated polymer and different incorporated polymers are summarized in Table I.

In the case of heating of the melt-quenched specimens from room temperature, the $T_{cc}(O)$, $T_{cc}(P)$, and $T_{cc}(E)$ values of the PLLA films with no incorporated polymer and different incorporated polymers increased in the following order: P(L-2HB)/P(D-2HB) < P(D-2HB) < P(L-2HB) < none, with the exception of $T_{cc}(O)$ of the PLLA film with P(D-2HB). For achieving uniformity in the present study, the incorporated polymer with the higher nucleating or crystallization-accelerating effect is shown on the left. In the case of cooling of the as-cast specimens from the melt, the $T_{cc}(O)$, $T_{cc}(P)$, and $T_{cc}(E)$ values decreased in the following order: P(D-2HB) > P(L-2HB)/P(D-2HB) > none > P(L-2HB). However, the normalized ΔH_{cc} values of PLLA homo-crystallites of the PLLA films with P(2HB) polymers are comparable to those of the PLLA film with no incorporated polymer. This is indicative of the fact that the incorporated P(2HB) polymers have almost no significant effect on the resultant crystallinity. That is, only the T_{cc} values were affected by the incorporated P(2HB) polymers. The crystallization of PLLA homo-crystallites in the PLLA film with P(L-2HB) was accelerated during heating and delayed during cooling. In addition, the effects of P(L-2HB)/P(D-2HB) HMSC crystallites in the PLLA film with P(L-2HB)/P(D-2HB) are relatively large for heating and small for cooling.

The relative crystallinity of PLLA of the specimens (X_r) was estimated using the following equation and are shown in Figure 2:

$$X_r(\%) = 100 \int_0^t (dH_{cc}/dt)dt \Big/ \int_0^\infty (dHcc/dt)dt, \quad (3)$$

where dH_{cc} denotes the measured enthalpy of (cold) crystallization during an infinitesimal time interval dt. In the case of the PLLA film with P(D-2HB), only the crystallization peaks below 132°C are used for

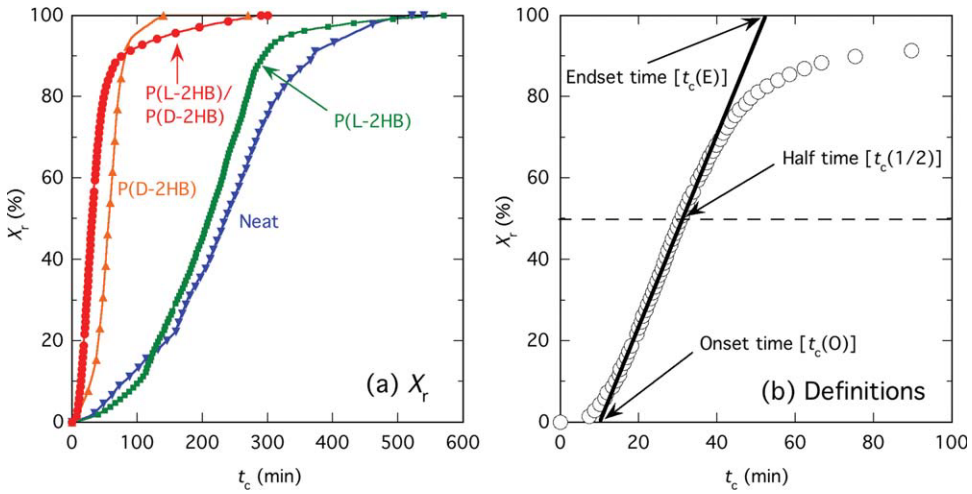

Figure 3 Relative crystallinity (X_r) of PLLA films with no incorporated polymer, P(L-2HB), P(D-2HB), and P(L-2HB)/P(D-2HB) crystallized at crystallization temperature (T_c) = 135°C as a function of crystallization time (t_c) (a) and X_r of PLLA film with P(L-2HB)/P(D-2HB) crystallized at crystallization temperature (T_c) = 135°C, where onset, half, and endset crystallization times [$t_c(O)$, $t_c(1/2)$, and $t_c(E)$, respectively] are defined (b). [Color figure can be viewed in the online issue, which is available at wileyonlinelibrary.com.]

the calculation of X_r. The X_r values thus calculated were used in the following Avrami analysis.

Isothermal crystallization

In contrast to nonisothermal crystallization where information is applicable to actual processing, the information for isothermal crystallization can be effectively used to estimate the crystallization rate and elucidate the crystallization mechanism in the presence of P(2HB) polymers. The overall crystallization behavior of the PLLA films with no incorporated polymer and different incorporated polymers was estimated by measuring the time change in the light intensity transmitted through the specimens (I) using polarized optical microscopy. The transmitted light intensity increased with an increase in crystallinity and finally leveled off when crystallization was complete. We used the relative light intensity defined by the following equation as an index of relative crystallinity (X_r):[30]

$$X_r(\%) = 100(I_t - I_0)(I_\infty - I_0), \quad (4)$$

where I_t and I_0 are the I values at crystallization time (t_c) = t and 0, respectively, and I_∞ is the I value at the plateau. Figure 3(a) shows the change in X_r in the PLLA films with different incorporated polymers at T_c = 135°C, as a function of t_c. Figure 3(b) shows the change in X_r in the PLLA film with P(L-2HB)/

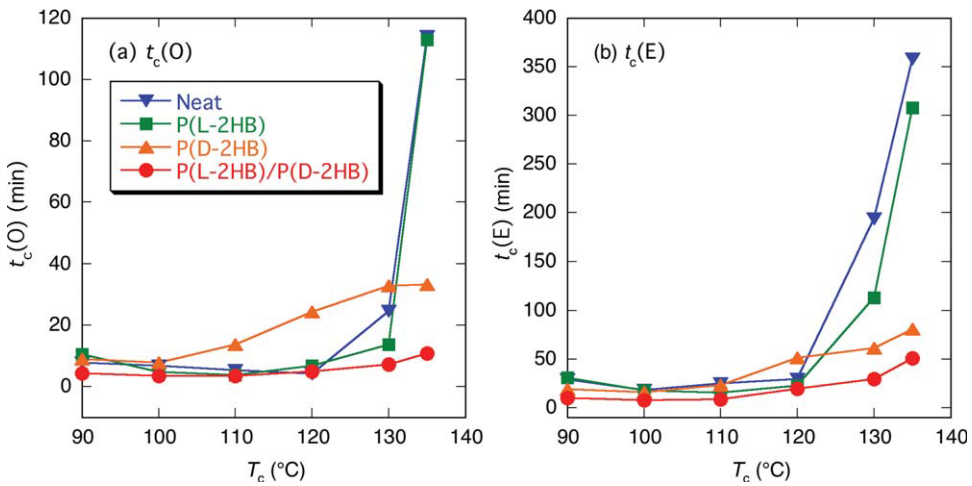

Figure 4 Onset and endset crystallization times [$t_c(O)$ and $t_c(E)$, respectively] of PLLA films with no incorporated polymer, P(L-2HB), P(D-2HB), and P(L-2HB)/P(D-2HB) as a function of crystallization temperature (T_c). [Color figure can be viewed in the online issue, which is available at wileyonlinelibrary.com.]

TABLE II
Avrami Exponent (n) and Crystallization Rate Constant (k) of PLLA Films with Different Incorporated Polymers

		Incorporated polymer						
Crystallization	Monitoring method	Type	Content (wt %)	T_c (°C)/scanning direction	n	k (min^{-n})	t_c (1/2) (min)	t_c (1/2) (Cal.)[a] (min)
Isothermal	Light intensity	Not added	0	90	2.89	1.65×10^{-4}	18.4	17.9
				100	3.85	4.75×10^{-5}	12.4	12.1
				110	2.25	1.52×10^{-3}	15.2	15.2
				120	1.63	6.09×10^{-3}	16.7	18.3
				130	1.53	4.55×10^{-4}	108.0	120.3
				135	1.42	2.01×10^{-4}	235.3	309.9
				Averaged	2.26			
		P(L-2HB)	10	90	2.93	9.15×10^{-5}	20.5	21.1
				100	1.83	5.65×10^{-3}	11.1	13.8
				110	2.53	2.37×10^{-3}	9.5	9.4
				120	3.09	1.93×10^{-4}	14.1	14.1
				130	2.03	1.77×10^{-4}	63.5	58.9
				135	2.26	3.42×10^{-6}	210.2	222.9
				Averaged	2.45			
		P(D-2HB)	10	90	3.90	2.05×10^{-5}	14.0	14.5
				100	3.58	7.98×10^{-5}	11.8	12.6
				110	2.68	1.62×10^{-4}	18.4	22.6
				120	1.78	7.22×10^{-4}	37.7	47.4
				130	3.71	3.21×10^{-7}	46.8	51.0
				135	2.10	9.09×10^{-5}	56.8	70.6
				Averaged	2.96			
		P(L-2HB)/P(D-2HB)	5/5	90	5.23	2.92×10^{-5}	7.2	6.9
				100	3.61	1.06×10^{-3}	5.5	6.0
				110	4.26	4.02×10^{-4}	6.0	5.8
				120	2.85	6.25×10^{-4}	12.2	11.7
				130	2.64	3.42×10^{-4}	18.4	17.9
				135	2.61	1.14×10^{-4}	30.8	28.2
				Averaged	3.53			
Nonisothermal	DSC	Not added	0	107–116/heating[b]	3.12	6.20×10^{-2}	–	–
				122–113/cooling[c]	3.05	5.38×10^{-5}	–	–
		P(L-2HB)	10	98–107/heating[b]	3.13	4.88×10^{-2}	–	–
				117–111/cooling[c]	2.93	1.78×10^{-4}	–	–
		P(D-2HB)	10	92–101/heating[b]	2.93	5.51×10^{-2}	–	–
				125–122/cooling[c]	5.68	5.74×10^{-7}	–	–
		P(L-2HB)/P(D-2HB)	5/5	92–99/heating[b]	3.37	7.44×10^{-2}	–	–
				126–118/cooling[c]	2.90	1.03×10^{-4}	–	–

[a] The values were estimated from eq. (8).
[b] T_0 values were set to 99.5, 89.4, 83.9, and 84.6°C for the PLLA films with no incorporated polymer, P(L-2HB), P(D-2HB), and P(L-2HB)/P(D-2HB), respectively. The values were estimated using the $[-\ln (1 - X_r/100)]$ values of 0.05–0.1 because of their nonlinear behavior above 0.1.
[c] T_0 values were set to 129.3, 123.0, 132.2, and 132.6°C for the PLLA films with no incorporated polymer, P(L-2HB), P(D-2HB), and P(L-2HB)/P(D-2HB), respectively.

P(D-2HB) crystallized at the same T_c, where the onset, half, and endset times for overall PLLA crystallization [$t_c(O)$, $t_c(1/2)$, and $t_c(E)$, respectively] are defined. The values of $t_c(O)$ and $t_c(E)$ were estimated by extrapolation of a line tangential to X_r to 0 and 100%, respectively. The values of $t_c(O)$ and $t_c(E)$ thus estimated are plotted in Figure 4 as a function of T_c. The $t_c(1/2)$ values are listed in Table II. The values of $t_c(O)$, $t_c(1/2)$, and $t_c(E)$ for all specimens increased with an increase in T_c. Such increases were remarkable for T_c exceeding 120°C. The increases in these values for T_c exceeding 120°C were large for the PLLA films with no incorporated polymer and P(L-2HB) than for the PLLA films with P(D-2HB) and P(L-2HB)/P(L-2HB).

For all T_c values, the PLLA film with P(L-2HB)/P(D-2HB) had the lowest $t_c(O)$, $t_c(1/2)$, and $t_c(E)$ values, reflecting the highly accelerated crystallization of PLLA homo-crystallites in the presence of P(L-2HB)/P(D-2HB) HMSC crystallites. In addition, although the $t_c(O)$ values of the PLLA film with P(D-2HB) was highest among the specimens for the T_c value range of 100–130°C, its $t_c(1/2)$ value for T_c = 90, 130, and 135°C and $t_c(E)$ for T_c = 90, 100, 130,

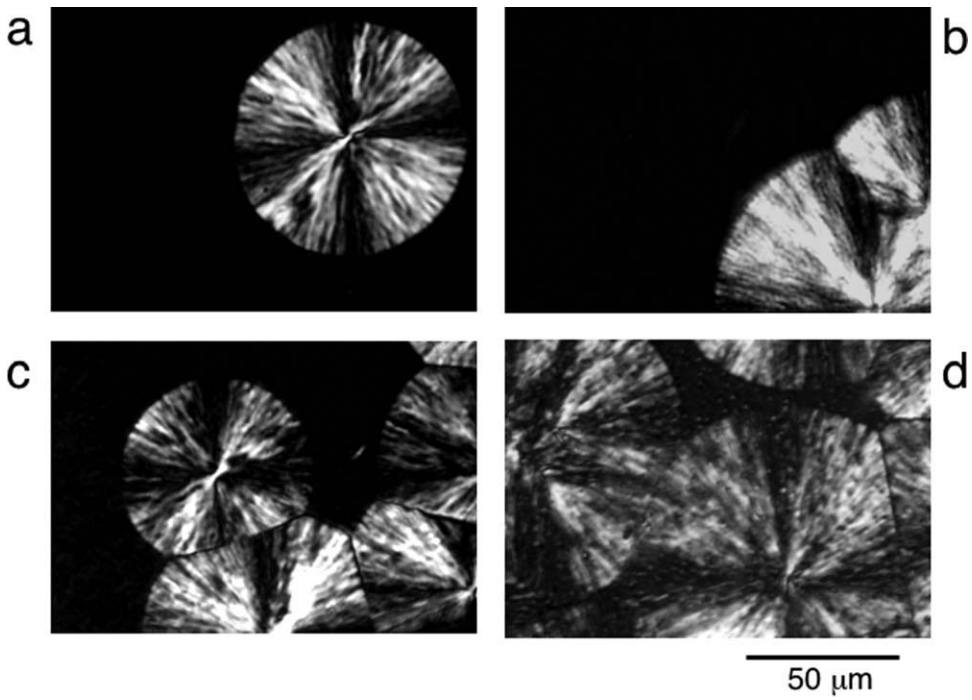

Figure 5 Polarized optical photomicrographs of PLLA films with no incorporated polymer (a) (t_c = 1562 s), (b) P(L-2HB) (t_c = 1800 s), (c) P(D-2HB) (t_c = 1814 s), and (d) P(L-2HB)/P(D-2HB) (t_c = 1800 s) crystallized at T_c = 130°C.

and 135°C was the second lowest among the specimens. This means that there is a relatively large accelerating effect when using P(D-2HB) in PLLA homo-crystallization, especially at relatively high and low-T_c values after the onset of PLLA homo-crystallization. The highest $t_c(O)$ values of the PLLA film with P(D-2HB) in the T_c range of 110–130°C indicate that the nucleation of PLLA homo-crystallites was disturbed by the presence of P(D-2HB). As seen from Figure 4(a), this disturbance effect on nucleation of PLLA homo-crystallites was higher for D-form P(D-2HB) than for L-form P(L-2HB). This indicates that the interaction between P(D-2HB) and PLLA having opposite configurations is higher than that between P(L-2HB) and PLLA having identical configurations. A similar result was reported for PLA and phenyl-substituted PLA.[43] Furthermore, $t_c(1/2)$ and $t_c(E)$ of the PLLA film with P(L-2HB) for T_c = 130 and 135°C were second highest among the specimens. This indicates that there was a very low, but nonetheless significant, crystallization-accelerating effect from P(L-2HB) at these relatively high-T_c values. The $t_c(O)$ value for T_c = 135°C and $t_c(1/2)$ and $t_c(E)$ for T_c = 130 and 135°C increased in the following order: P(L-2HB)/P(D-2HB) < P(D-2HB) < P(L-2HB) < none. This order is in agreement with that of the T_{cc} values during heating.

To investigate the isothermal crystallization behavior in detail, the spherulite growth behavior was monitored by polarized optical microscopy. Figure 5 shows the polarized optical photomicrographs of the PLLA films with no incorporated polymer and different incorporated polymers. Maltese crosses were seen for all PLLA films (reflecting the formation of relatively well-oriented lamellae in the spherulites) regardless of the incorporated polymers. However, the PLLA film with P(L-2HB)/P(D-2HB) had numerous white spots of small crystallites both inside and outside the spherulites of PLLA homo-crystallites. These spots should be the P(L-2HB)/P(D-2HB) HMSC crystallites, and probably because of their presence, the spherulite number per unit mass was elevated. In addition, in the PLLA film with P(D-2HB), the spherulite number per unit mass was elevated compared to that of the PLLA film with no incorporated polymer. The spherulite densities or nucleating effects of incorporated polymers decreased in the following order: P(L-2HB)/P(D-2HB) > P(D-2HB) > P(L-2HB), none.

The radial spherulite growth rate (G) of PLLA homo-crystallites was evaluated using the polarized optical photomicrographs for different T_c values and is plotted in Figure 6 as a function of T_c. The G values of the PLLA film with no incorporated polymer were lowest; maximum G values of $\sim$ 1.5 μm min^{-1} were obtained at T_c values of 120 and 130°C. The G values of the PLLA film with P(L-2HB) or P(D-2HB) showed a similar T_c dependence to that of the PLLA film with no incorporated polymer and were 0.3–0.4 μm min^{-1} higher than those of the PLLA film with no incorporated polymer. The G values of the PLLA film with P(L-2HB)/P(D-2HB) were constant at

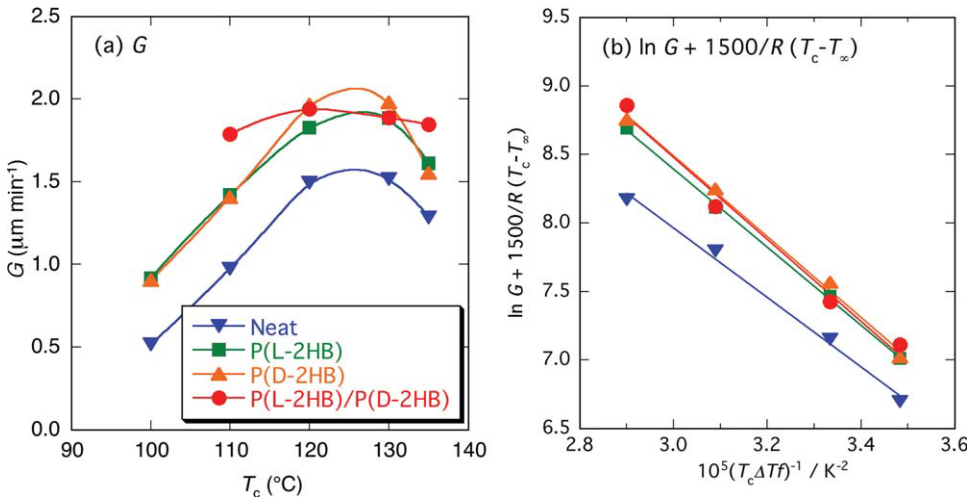

Figure 6 Radial spherulite growth rate (G) (a) and $\ln G + 1500/R(T_c - T_\infty)$ (b) of PLLA films with no incorporated polymer, P(L-2HB), P(D-2HB), and P(L-2HB)/P(D-2HB) as functions of T_c and $1/(T_c\Delta T_f)$, respectively. [Color figure can be viewed in the online issue, which is available at wileyonlinelibrary.com.]

around 1.9 μm min^{-1} and were 0.4–0.8 μm min^{-1} higher than those of the PLLA film with no incorporated polymer. The G values of the PLLA films with no incorporated polymer and different incorporated polymers decreased in the following order: P(L-2HB)/P(D-2HB) $\geq$ P(L-2HB), P(D-2HB) $>$ none. The value of T_c for the PLLA films (Fig. 6) was the same as or higher than the value of T_m for P(L-2HB) or P(D-2HB) homo-crystallites ($\sim$ 100°C). This means that P(L-2HB) or P(D-2HB) was in a molten state and should have acted as a diluent, which would have disturbed the diffusion of PLLA chains to crystalline growth sites or acted as a plasticizer, which would have enhanced the mobility of PLLA and accelerated the segmental diffusion to the crystalline growth sites. The elevated G values of the PLLA films with P(2HB) indicate that P(L-2HB) and P(D-2HB) acted as plasticizers rather than as diluents.

Crystallization mechanism

Overall, crystallization kinetics traced by DSC in nonisothermal crystallization and by measuring light intensity in isothermal crystallization was analyzed according to the Avrami theory,[44–46] which is expressed by the following equation:

$$1 - X_r(\%)/100 = \exp(-kt_c^n), \tag{5}$$

where k is the crystallization rate constant. Equation (5) can be transformed to eq. (6):

$$\ln[-\ln\,(1 - X_r/100)] = \ln\;k + n\ln t_c. \tag{6}$$

In the case of nonisothermal crystallization during heating or cooling, t_c is the crystallization time and is defined by the following equation:

$$t_c = |T_c - T_0|/\Phi, \tag{7}$$

where T_0 is the T_c at which PLLA homo-crystallization started and Φ (K, min^{-1}) is the heating or cooling rate. Here, the T_0 values were T_c values at which X_r values showed a significant increase (0.1%). For the heating process, T_0 values were set to 99.5, 89.4, 83.9, and 84.6°C for the PLLA films with no incorporated polymer, P(L-2HB), P(D-2HB), and P(L-2HB)/P(D-2HB), respectively. During the cooling process, T_0 values were set to 129.3, 123.0, 132.2, and 132.6°C for the PLLA films with no incorporated polymer, P(L-2HB), P(D-2HB), and P(L-2HB)/P(D-2HB), respectively. In the exceptional case of the PLLA film with P(D-2HB) during cooling, the crystallization peaks at around 120 and 140°C are assumed to be those of PLLA homo-crystallites and P(D-2HB)/PLLA HTSC crystallites, respectively. However, in this case, only the X_r of PLLA homo-crystallites was estimated. The plots, according to eq. (6), for nonisothermal crystallization (heating and cooling) and isothermal crystallization are given in Figure 7. From these plots, the slope (n) and the intercept (k) were obtained. To avoid the effect of the noise level of X_r below 3% on the base line and avoid deviation from the theoretical curves, as noted by Mandelkern,[47] for X_r exceeding 25%, we used the data for X_r in the range of 3–25% for estimating the n and k values. Linear dependence of $\ln[-\ln\,(1 - X_r/100)]$ on $\ln\,t_c$ was observed in all the plots. In addition, the $t_c(1/2)$ for PLLA crystallization was calculated using the following equation:

$$t_c(1/2)(\text{Cal.}) = [(\ln\;2)/\text{k}]^{1/\text{n}}. \tag{8}$$

The values of n, k, and $t_c(1/2)$ (Cal.) thus obtained are summarized in Table II.

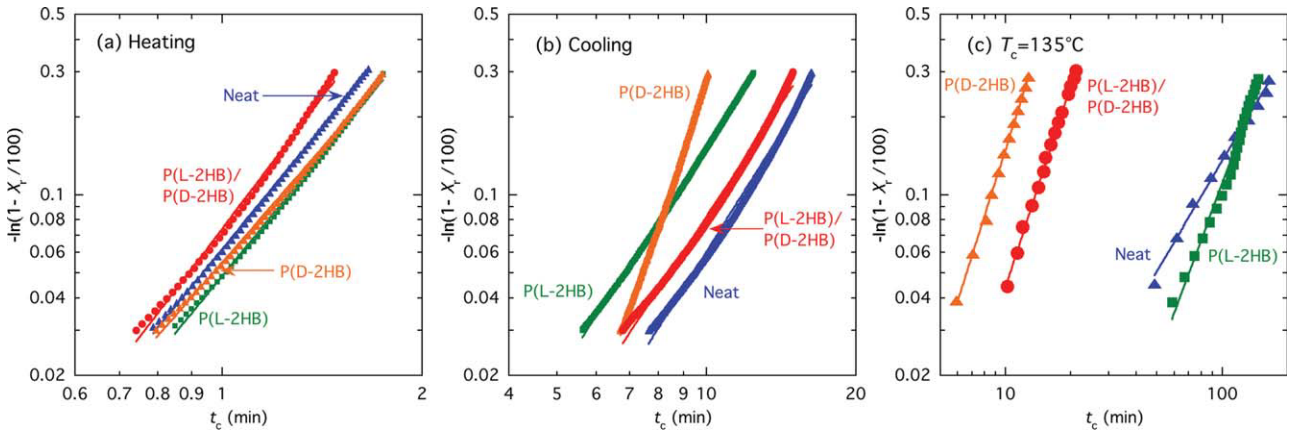

Figure 7 ln (1 − X_r/100) of PLLA films with no incorporated polymer, P(L-2HB), P(D-2HB), and P(L-2HB)/P(D-2HB) during heating (a), cooling (b), and crystallization at T_c = 135°C (c) as a function of crystallization time (t_c). [Color figure can be viewed in the online issue, which is available at wileyonlinelibrary.com.]

For nonisothermal crystallization (heating and cooling), all n values are ~ 3, with the exception of the PLLA film with P(D-2HB), where P(D-2HB)/PLLA HTSC crystallites were formed before the occurrence of PLLA homo-crystallization (with a value of 5.7). As reported elsewhere, in the case of sporadic nucleation with n values of 2, 3, 4, and 6 or higher, the crystallite growth units formed are a fibril, a disc, spherulites, and a sheaf, respectively. However, in the case of rapid nucleation in which growth centers are formed at the same time, the corresponding values of the exponent would be (n − 1).[48] Assuming rapid nucleation, n values of 3 (=4 − 1) for most specimens result in spherulitic growth, whereas the relatively large n value of the PLLA film with P(D-2HB) (of 5.7) is 5 (=6 − 1) or higher and thus suggests sheaflike growth of PLLA homo-crystallites in the presence of P(D-2HB)/PLLA HTSC crystallites. These findings indicate that only the presence of P(D-2HB)/PLLA HTSC crystallites altered the growth mechanism of PLLA homo-crystallites. In isothermal crystallization, n values are in the ranges of 1.4–3.9, 1.8–3.1, 1.8–3.9, and 2.6–5.2. Averaged n values are 2.3, 2.5, 3.0, and 3.5 for the PLLA films with no incorporated polymer, P(L-2HB), P(D-2HB), and P(L-2HB)/P(D-2HB), respectively. As listed in Table II, n or the crystallization mechanism depends on the type of incorporated polymer and T_c. The n values tend to have higher values with decreasing T_c.

Hoffman analysis

To further investigate the crystallization kinetics, we estimated the nucleation constant (K_g) and the front constant (G_0) of the specimens using the nucleation theory established by Hoffman and Lauritzen,[49,50] where G can be expressed by the following equation:

$$G = G_0 \exp[-U^*/R(T_c - T_\infty)] \exp[-K_g/(T_c \Delta T_f)], \quad (9)$$

where ΔT is $T_m^0 - T_c$ (supercooling) when T_m^0 is equivalent to the equilibrium value of T_m; f is a factor expressed by $2T_c/(T_m^0 + T_c)$, which accounts for the change in the heat of fusion as the temperature falls below T_m^0; U^* is the activation energy for the transportation of segments to the crystallization site; R is the gas constant; and T_∞ is the hypothetical temperature where all motion associated with viscous flow ceases. Figure 6(b) illustrates the [ln G + $1500/R(T_c - T_\infty)$] values of PLLA films with no incorporated polymer and different incorporated polymers as a function of $1/(T_c \Delta T_f)$, assuming that the specimens are composed only of PLLA and that T_m^0 is 212°C.[51] Here, we used the universal values of U^* = 1500 cal mol^{-1} and $T_\infty = T_g - 30$ K for comparison with the reported values.[52–55] The plots in Figure 6(b) give K_g as the slope and ln G_0 as the intercept. The values of K_g and G_0 thus estimated are summarized in Table III.

The estimated K_g values of all specimens are very similar to each other and are in the range of 2.6–3.0 × 10^5 K^2, which are consistent with the reported ones for regime II (1.9–3.5 × 10^5 K^2).[52–55] These findings show that the nucleation of PLLA homo-crystallites in all specimens proceeds via the regime II mechanism and is not altered by the incorporation of P(2HB) polymers. The obtained G_0 values (6.0 × 10^6 − 4.0 × 10^7 μm min^{-1}) are also consistent with those reported for regime II (1.8–4.0 × 10^7 μm min^{-1}).[55]

Crystalline species before crystallization

To determine the type of crystallites formed before isothermal crystallization and nonisothermal crystallization with heating from 0°C or cooling from the melt, we prepared melt-quenched specimens, and their WAXS measurements were performed

TABLE III
Estimated Front Constant (G_0) and Nucleation Constant (K_g)

Incorporated polymer			
Type	Content (wt %)	G_0(II)[a] ($\mu m\ min^{-1}$)	K_g (II)[a] (K^2)
Not added	0	5.96×10^6	2.54×10^5
P(L-2HB)	10	2.19×10^7	2.85×10^5
P(D-2HB)	10	3.26×10^7	2.94×10^5
P(L-2HB)/P(D-2HB)	5/5	3.98×10^7	2.99×10^5

[a] (II) indicates regime II.

[Fig. 8(a)]. Evidently, no melt-quenched specimens showed crystalline diffractions of PLLA homo-crystallites, reflecting the absence of PLLA homo-crystallites before the occurrence of the isothermal and nonisothermal crystallization. In contrast, the crystalline diffraction peaks of P(L-2HB) homo-crystallites (main peak at 14.8°), P(D-2HB) homo-crystallites (main peak at 14.8°), and P(L-2HB)/P(D-2HB) HMSC crystallites (main peak at 10.8°) were observed for the melt-quenched PLLA films with P(L-2HB), P(D-2HB), and P(L-2HB)/P(D-2HB), respectively.[39] This indicates that P(L-2HB) or P(D-2HB) homo-crystallites and P(L-2HB)/P(D-2HB) HMSC crystallites were present during both isothermal crystallization and nonisothermal crystallization with heating in the T_c range from 0°C up to their T_m values (~ 100 and 203°C, respectively, see Table I). The P(L-2HB) or P(D-2HB) homo-crystallites were formed during the quenching process. However, it should be noted that the P(L-2HB)/P(D-2HB) HMSC crystallites were formed during the solvent-casting process and remained unmelted during the melt quenching of the PLLA phase and were acting as nucleating agents for all crystallization processes (isothermal and nonisothermal crystallization).

To further investigate the crystalline species formed after crystallization, WAXS measurements were performed for the specimens that were cooled slowly at a constant rate of -1°C min^{-1} from the melt to room temperature [Fig. 8(b)]. The crystalline peaks of solely PLLA homo-crystallites (main peak at 16.8°) were noticed for the PLLA film with no incorporated polymer.[56] In contrast, in addition to the crystalline peaks of PLLA homo-crystallites, the PLLA films with P(L-2HB), P(D-2HB), and P(L-2HB)/P(D-2HB) had P(L-2HB) homo-crystallites (main peak at 14.8°), P(D-2HB)/PLLA HTSC crystallites (main peak at 11.2°),[40] and P(L-2HB)/P(D-2HB) HMSC crystallites (main peak at 10.8°), respectively. As the P(D-2HB)/PLLA HTSC crystallites were not observed for melt-quenched PLLA film with P(D-2HB), this film had no P(D-2HB)/PLLA HTSC crystallites before isothermal crystallization and nonisothermal crystallization with cooling. Therefore, the exothermic peak observed at ~ 140°C of the PLLA film with P(D-2HB) during cooling [Fig. 1(b)] is confirmed to be due to the crystallization of P(D-2HB)/PLLA HTSC crystallites. On the other hand, the relative intensities of the crystalline peaks of P(L-2HB) homo-crystallites after having been slowly cooled from the melt were similar to those of the melt-quenched PLLA film with P(L-2HB). This suggests that slow cooling will not induce greater P(L-2HB) homo-crystallization than that caused by the rapid cooling of melt quenching. The PLLA film with P(L-2HB) included P(L-2HB) homo-crystallites during isothermal crystallization below its T_m and during heating to its T_m.

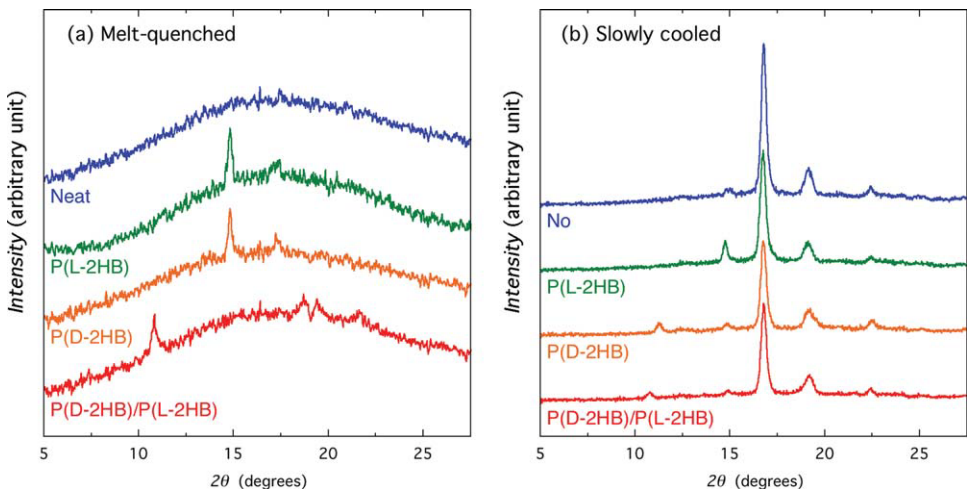

Figure 8 WAXS profiles of PLLA films with no incorporated polymer, P(L-2HB), P(D-2HB), and P(L-2HB)/P(D-2HB) that were melt quenched (a) and cooled at -1°C min^{-1} from the melt (b). [Color figure can be viewed in the online issue, which is available at wileyonline library.com.]

DISCUSSION

Factors affecting crystallization rate

Accelerated crystallization of PLLA homo-crystallites occurred during heating in the presence of P(L-2HB), P(D-2HB), and P(L-2HB)/P(D-2HB); during cooling in the presence of P(D-2HB) and P(L-2HB)/P(D-2HB); and during isothermal crystallization in the presence of P(L-2HB) or P(L-2HB) for T_c of 130 and 135°C and in the presence of P(L-2HB)/P(D-2HB) for T_c in the range of 90–135°C. As summarized in the previous work,[32] the resultant effects of an incorporated second polymer on PLLA homo-crystallization can be classified on the basis of (1) spherulite (or crystallite) nuclei per unit mass, (2) G, and (3) induction period. The third effect is added to those in the literature.[32] These effects basically depend on the factors of (1) the miscibility of PLLA with the second polymer (or the dilution effect); (2) the direct nucleating ability or nucleation-assisting ability of the second polymer, which is affected by the state of the second polymer (in the crystalline or in the noncrystalline state); and (3) the chain mobility of PLLA at T_c, which depends on the T_g value of the second polymer relative to that of PLLA. In a miscible or partially miscible system, the dilution effect of the second polymer will lower the driving force for the formation of crystalline nuclei of PLLA homo-crystallites. The second polymer can be a steric obstacle to the diffusion of PLLA chains to the crystallite growth sites or self-nucleating sites. This will delay the nucleation and growth of the PLLA homo-crystallites (or spherulites). Essentially, this will decrease the G and number of spherulite nuclei per unit mass of PLLA homo-crystallites and increase the induction period for the formation of spherulite (crystallites) nuclei. However, if PLLA that is miscible with the second polymer has a T_g value lower than that of PLLA, the second polymer will increase the chain mobility of PLLA and thereby assist the self-nucleation and growth of PLLA homo-crystallites. Specifically, this will increase G and the number of spherulite nuclei per unit mass of PLLA homo-crystallites and decrease the induction period for the formation of spherulite (crystallites) nuclei. Therefore, the net effect of the second polymers is determined by the counterbalance between the two effects of disturbance and assistance.

In the present study, although P(L-2HB) and P(D-2HB) have relatively low T_g ($\sim$ 25°C),[39] the T_g values of the PLLA films with P(L-2HB), P(D-2HB), and P(L-2HB)/P(D-2HB) (50, 50, and 49°C, respectively) were the same as that of the PLLA film with no incorporated polymer (48°C). This suggests that the chain mobility traced by T_g was not elevated by the presence of P(2HB) polymers. However, no significant change in T_g can be ascribed to the small amount of P(2HB) polymers in the specimens. The effect of elevated molecular mobility in the presence of incorporated P(2HB) polymers was indicated by the increase in the G values of the PLLA films with P(2HB) polymers (Fig. 7), which might have increased the total crystallization rate. The state of materials, solid or melt, is crucial for determining the nucleating effect. Although the interfaces between PLLA melt and P(2HB) melt can act as nucleating sites for PLLA, solid-state nucleation agents, that is, P(L-2HB) or P(D-2HB) homo-crystallites, P(D-2HB)/PLLA HTSC crystallites, and P(L-2HB)/P(D-2HB) HMSC crystallites should be more effective.

Nonisothermal crystallization

For nonisothermal crystallization during heating, as shown in Figure 8(a), P(L-2HB) or P(D-2HB) homo-crystallites and P(L-2HB)/P(D-2HB) HMSC crystallites were present for T_c values from room temperature up to their T_m values of $\sim$ 100 and 203°C, respectively. Therefore, the finding that T_{cc}(O) values of the PLLA films with P(2HB) polymers during heating were lower than that of the PLLA film with no incorporated polymer strongly suggests that P(2HB) homo-crystallites and P(L-2HB)/P(D-2HB) HMSC crystallites acted as nucleating agents for PLLA homo-crystallites. The nucleating effect of P(L-2HB)/P(D-2HB) HMSC crystallites was higher than that of P(L-2HB) or P(D-2HB) homo-crystallites. In addition, the nucleating effect of D-form P(2HB) homo-crystallites [that is, P(D-2HB) homo-crystallites] was higher than that of L-form P(2HB) homo-crystallites [that is, P(L-2HB) homo-crystallites].

For nonisothermal crystallization with cooling, the highest T_{cc} values of PLLA homo-crystallites observed for the PLLA film with P(D-2HB) should be because of the highest nucleating effect of P(D-2HB)/PLLA HTSC crystallites formed during cooling at around 140°C [Fig. 1(a)]. In contrast, based on the T_m value of P(L-2HB) ($\sim$ 100°C), the PLLA film with P(L-2HB) as well as that with no incorporated polymer had no crystallites as nucleating agents before the crystallization of PLLA homo-crystallites. In the case of the PLLA film with P(L-2HB), the presence of P(L-2HB) melt is thought to have disturbed nucleation and the growth of PLLA homo-crystallites, resulting in the lowest T_{cc} values and a broad crystallization peak among the specimens.

A comparison between Figure 1(a,b) shows that the nucleating effect of P(L-2HB)/P(D-2HB) HMSC crystallites was higher for heating at low temperature than for cooling at high temperature. Although, the crystallization of PLLA homo-crystallites in the PLLA film with P(L-2HB) was accelerated during heating because of the presence of P(L-2HB) homo-crystallites and delayed during cooling because of

both the absence of P(L-2HB) homo-crystallites and the diluting effect of P(L-2HB). This confirms that the P(L-2HB) homo-crystallites present during heating up to 100°C acted as nucleating agents. The same nucleating effect was observed for P(D-2HB) homo-crystallites during heating. However, it should be noted that the nucleating agents of the PLLA film with P(D-2HB) differ between cooling and heating processes. That is, for cooling, the nucleating agent is P(D-2HB)/PLLA HTSC crystallites, and, for heating, the nucleating agent is P(D-2HB) homo-crystallites.

Isothermal crystallization

The WAXS results of the melt-quenched specimens showed that only P(L-2HB)/P(D-2HB) HMSC crystallites in the PLLA film with P(L-2HB)/P(D-2HB) existed as nucleating crystalline species before isothermal crystallization, with the exception of P(L-2HB) or P(D-2HB) homo-crystallites, which can be formed for T_c values below 100°C. The nucleating effect of the P(L-2HB)/P(D-2HB) HMSC was highest among the specimens for all T_c values and became remarkably high for the high T_c values of 130 and 135°C. However, P(D-2HB)/PLLA HTSC crystallites and P(2HB) homo-crystallites that had been formed during isothermal crystallization for the T_c range below 140 and 100°C, respectively, could act as nucleating agents. The very high-$t_c(O)$ values for the PLLA film with P(D-2HB) in the T_c range of 110–130°C [Fig. 4(a)] strongly suggest that P(D-2HB) acted as a diluent of PLLA and disturbed the self-nucleation of PLLA homo-crystallites at an early stage. However, the relatively low-$t_c(O)$ values for the T_c value of 135°C and $t_c(1/2)$ and $t_c(E)$ values for the T_c values of 130 and 135°C that were observed for the PLLA film with P(D-2HB) suggest that the P(D-2HB)/PLLA HTSC crystallites acted as nucleating agents after their formation and that the incorporated free P(D-2HB) chains increased the G values (Fig. 6), resulting in the elevated overall crystallization rate. For the T_c range of 110–130°C, $t_c(E)$ values of the PLLA film with P(D-2HB) were similar to those of other specimens, probably because the nucleation effect of P(D-2HB)/PLLA HTSC crystallites and the increase in G were not remarkably high.

On the other hand, $t_c(O)$ of the PLLA film with P(L-2HB) was similar to that of the pure PLLA film. This indicates that the incorporated P(L-2HB) had no significant effect on the nucleation of PLLA homo-crystallites. However, the $t_c(1/2)$ and $t_c(E)$ values of the PLLA film with P(L-2HB) for the relatively high-T_c values of 130 and 135°C were significantly lower that those of the PLLA film with no incorporated polymer. This faster completion of PLLA homo-crystallization in the PLLA film with P(L-2HB) compared to that with no incorporated polymer is attributable to the higher G values (Fig. 6).

The present study examined P(L-2HB)/P(D-2HB) HMSC crystallites, P(D-2HB)/PLLA HTSC crystallites, and P(L-2HB) or P(D-2HB) homo-crystallites and found them to be promising biodegradable nucleating agents for PLLA homo-crystallization to prepare all biodegradable PLLA-based materials. The P(L-2HB)/P(D-2HB) HMSC crystallites are most effective during nonisothermal crystallization and nonisothermal crystallization with heating, whereas the P(D-2HB)/PLLA HTSC crystallites are most effective during nonisothermal crystallization with cooling from the melt. However, further detailed study is required for determining the factor dominating PLLA homo-crystallization for each specimen under different crystallization conditions.

CONCLUSIONS

Accelerated crystallization of PLLA homo-crystallites occurred during heating in the presence of P(L-2HB), P(D-2HB), and P(L-2HB)/P(D-2HB); during cooling in the presence of P(D-2HB) and P(L-2HB)/P(D-2HB); and during isothermal crystallization in the presence of P(L-2HB) or P(D-2HB) for T_c of 130 and 135°C and in the presence of P(L-2HB)/P(D-2HB) for T_c in the range of 90–135°C. The accelerating effects of incorporated polymers decreased in the following orders: P(L-2HB)/P(D-2HB) > P(D-2HB) > P(L-2HB) > none, for heating and isothermal crystallization for T_c of 130 and 135°C and P(D-2HB) > P(L-2HB)/P(D-2HB) > none > P(L-2HB), for cooling. In the case of cooling, the presence of P(L-2HB) disturbed PLLA homo-crystallization.

The P(L-2HB)/P(D-2HB) HMSC crystallites, P(D-2HB)/PLLA HTSC crystallites, and P(L-2HB) or P(D-2HB) homo-crystallites are found to be promising biodegradable nucleating agents for PLLA homo-crystallization to prepare all biodegradable PLLA-based materials. The P(L-2HB)/P(D-2HB) HMSC crystallites are most effective during isothermal crystallization and nonisothermal crystallization with heating, whereas the P(D-2HB)/PLLA HTSC crystallites are most effective during nonisothermal crystallization with cooling from the melt. In addition to the nucleating effect, the plasticizing effect of free P(2HB) chains, which increases G and the PLLA spherulite number per unit mass, accelerates crystallization of PLLA homo-crystallites. In the case of the PLLA film with P(L-2HB) during cooling, crystallization is delayed compared to the case of PLLA film with no incorporated polymers. This can be ascribed to the dilution effect of P(L-2HB), which prolongs the spherulite nucleation and decreases the spherulite number per unit mass.

References

1. Auras, R.; Lim, L.-T.; Selke, S. E. M.; Tsuji, H., Eds. Poly(lactic acid): Synthesis, Structures, Properties, Processing, and Applications; Wiley: New Jersey, 2010.
2. Thakur, K. A. M.; Kean, R. T.; Zupfer, J. M.; Buehler, N. U.; Doscotch, M. A.; Munson, E. J. Macromolecules 1996, 29, 8844.
3. Kolstad, J. J. J Appl Polym Sci 1996, 62, 1079.
4. Schmidt, S. C.; Hillmyer, M. A. J Polym Sci Part B: Polym Phys 2001, 39, 300.
5. Nam, J. Y.; Ray, S. S.; Okamoto, M. Macromolecules 2003, 36, 7126.
6. Urayama, H.; Kanamori, T.; Fukushima, K.; Kimura, Y. Polymer 2003, 44, 45635.
7. Ray, S. S.; Yamada, K.; Okamoto, M.; Fujimoto, Y.; Ogami, A.; Ueda, K. Polymer 2003, 44, 6633.
8. Lee, J. H.; Park, T. G.; Park, H. S.; Lee, D. S.; Lee, Y. K.; Yoon, S. C.; Nam, J.-D. Biomaterials 2003, 24, 2773.
9. Pluta, M. Polymer 2004, 45, 8239.
10. Krikorian, V.; Pochan, D. J. Macromolecules 2005, 38, 6520.
11. Moon, S. I.; Jin, F.; Lee, C. J.; Tsutsumi, S.; Hyon, S. H. Macromol Symp 2005, 224, 287.
12. Nam, J. Y.; Okamoto, M.; Okamoto, H.; Nakano, M.; Usuki, A.; Matsuda, M. Polymer 2006, 47, 1340.
13. Tsuji, H.; Takai, H.; Fukuda, N.; Takikawa, H. Macromol Mater Eng 2006, 291, 325.
14. Tsuji, H.; Kawashima, Y.; Takikawa, H. J Polym Sci Part B: Polym Phys 2007, 45, 2167.
15. Li, H.; Huneault, M. A. Polymer 2007, 48, 6855.
16. Liao, R.; Yang, B.; Yu, W.; Zhou, C. J Appl Polym Sci 2007, 104, 310.
17. Pluta, M.; Murariu, M.; Ferreira, A. D. S.; Alexandre, M.; Galeski, A.; Dubois, P. J Polym Sci Part B: Polym Phys 2007, 45, 2770.
18. Tsuji, H.; Kawashima, Y.; Takikawa, H.; Tanaka, S. Polymer 2007, 48, 4213.
19. Harris, A. M.; Lee, E. C. J Appl Polym Sci 2008, 107, 2246.
20. Ozkoc, G.; Kemaloglu, S. J Appl Polym Sci 2009, 114, 2481.
21. Yuzay, I. E.; Auras, R.; Selke, S. J Appl Polym Sci 2010, 115, 2262.
22. Xiao, H. W.; Li, P.; Ren, X.; Jiang, T.; Yeh, J.-T. Appl Polym Sci 2010, 118, 3558.
23. Kawamoto, N.; Sakai, A.; Horikoshi, T.; Urushihara, T.; Tobita, E. J Appl Polym Sci 2007, 103, 198.
24. Kawamoto, N.; Sakai, A.; Horikoshi, T.; Urushihara, T.; Tobita, E. J Appl Polym Sci 2007, 103, 244.
25. Pan, P.; Zhu, B.; Dong, T.; Inoue, Y. J Polym Sci Part B: Polym Phys 2008, 46, 2222.
26. Pan, P.; Liang, Z.; Cao, A.; Inoue, Y. ACS Appl Mater Interfaces 2009, 1, 402.
27. Brochu, S.; Prud'homme, R. E.; Barakat, I.; Jérôme, R. Macromolecules 1995, 28, 5230.
28. Yamane, H.; Sasai, K. Polymer 2003, 44, 2569.
29. Anderson, K. S.; Hillmyer, M. A. Polymer 2006, 47, 2030.
30. Tsuji, H.; Takai, H.; Saha, S. K. Polymer 2006, 47, 3826.
31. Tsuji, H.; Tashiro, K.; Bouapao, L.; Narita, J. Macromol Mater Eng 2008, 293, 947.
32. Tsuji, H.; Sawada, M.; Bouapao, L. ACS Appl Mater Interfaces 2009, 1, 1719.
33. Slager, J.; Domb, A. J Adv Drug Delivery Rev 2003, 55, 549.
34. Tsuji, H. Macromol Biosci 2005, 5, 569.
35. Fukushima, K.; Kimura, K. Polym Int 2006, 55, 626.
36. Leevameng, B.; Tsuji, H. Macromol Chem Phys 2009, 210, 993.
37. Masutani, K.; Kawabata, S.; Aoki, T.; Kimura, Y. Polym Int 2010, 59, 1526.
38. Tsuji, H.; Tsuruno, T. Macromol Mater Eng 2010, 295, 709.
39. Tsuji, H.; Okumura, A. Macromolecules 2009, 42, 7263.
40. Tsuji, H.; Yamamoto, S.; Okumura, A.; Sugiura, Y. Biomacromolecules 2010, 11, 252.
41. Tsuji, H.; Matsuoka, H.; Itsuno, S. J Appl Polym Sci 2008, 110, 3954.
42. Tsuji, H.; Tezuka, Y. Biomacromolecules 2004, 5, 1181.
43. Tsuji, H.; Matsuoka, H. Macromol Rapid Commun 2008, 29, 1372.
44. Avrami, M. J Chem Phys 1939, 7, 1103.
45. Avrami, M. J Chem Phys 1940, 8, 212.
46. Avrami, M. J Chem Phys 1941, 9, 177.
47. Mandelkern, L. Crystallization of Polymers; McGraw-Hill: New York, 1964.
48. Cowie, J. M. G. Polymers: Chemistry and Physics of Modern Materials, 2nd ed.; Blackie Academic: Glasgow, UK; Chapter 11, p 229–246.
49. Hoffman, J. D.; Frolen, L. J.; Ross, G. S.; Lauritzen, J. I., Jr. J Res Natl Bur Stand A: Phys Chem 1975, 79, 671.
50. Hoffman, J. D.; Davis, G. T.; Lauritzen, J. I., Jr. In Crystalline and Non-Crystalline Solids; Treatise on Solid State Chemistry, Vol.3; Hannay, N. B., Ed.; Plenum: New York, 1976; Chapter 7, p 497–614.
51. Tsuji, H.; Ikada, Y. Polymer 1995, 36, 2709.
52. Vasanthakumari, R.; Pennings, A. J. Polymer 1983, 24, 175.
53. Abe, H.; Harigaya, M.; Kikkawa, Y.; Tsuge, T.; Doi, Y. Biomacromolecules 2005, 6, 457.
54. Di Lorenzo, M. L. Polymer 2001, 42, 9441.
55. Tsuji, H.; Miyase, T.; Tezuka, Y.; Saha, S. K. Biomacromolecules 2005, 6, 244.
56. Tsuji, H.; Nakano, M.; Hashimoto, M.; Takashima, K.; Katsura, S.Mizuno, A. Biomacromolecules 2006, 7, 3316.